Polymer Chemistry

Accepted Manuscript

ROYAL SOCIETY OF CHEMISTRY

www.rsc.org/polymers

Low Bandgap Poly(thienylenemethine) Derivatives Bearing Side Chain Terarylene Moieties

Sangbum Ahn, Kazuki Yabumoto, Yongsoo Jeong, and Kazuo Akagi*

Department of Polymer Chemistry, Kyoto University, Katsura, Kyoto 615-8510, Japan

EMAIL ADDRESS: akagi@fps.polym.kyoto-u.ac.jp

RECEIVED DATE (to be automatically inserted after your manuscript is accepted if required according to the journal that you are submitting your paper to)

TITLE RUNNING HEAD: Low Bandgap Poly(thienylenemethine)s

CORRESPONDING AUTHOR FOOTNOTE:

* Department of Polymer Chemistry, Kyoto University

ABSTRACT:

We designed and synthesised low bandgap poly(bithienylenemethine) and poly(terthienylenemethine) derivatives bearing arylene moieties in their side chains. These polymers consisted of alternating benzonoidal and quinoidal structures in the main chains. Arylene moieties were introduced in the side chains to stabilize the quinoidal structure of the polymers, because they are anticipated to delocalize π-conjugated electrons of the main chains over the side chains. The polymers were synthesised by polycondensation reactions between arylenes and aryl aldehydes using H_2SO_4, followed by oxidative dehydrogenation using 2,3-dichloro-5,6-dicyano-1,4-benzoquinone (DDQ). The quinoidal polymers showed absorption bands in the UV-visible and near infrared regions. The optically and electrochemically evaluated bandgaps of quinoidal poly(bithienylenemethine) with the terphenylene moiety in the side chain (**Poly-2PQ**) were 1.7 and 2.2 eV, respectively, and those of quinoidal poly(terthienylenemethine) with the terphenylene moiety in the side chain (**Poly-3PQ**) were 0.8 and 1.6 eV, respectively. Similarly, the optical and electrochemical bandgaps of quinoidal poly(bithienylenemethine) with the terthiophene side chain (**Poly-2TQ**) were 1.5 and 1.7 eV, respectively, and those of quinoidal poly(terthienylenemethine) with the terthiophene side chain (**Poly-3TQ**) were 0.8 and 1.2 eV, respectively. These low bandgap polymers are regarded as prospective candidate materials for plastic electronics, including organic solar cell devices.

KEYWORDS: benzonoidal and quinoidal structure, poly(thienylenemethine)s, low bandgap polymer, oxidative dehydrogenation

Introduction

Conjugated polymers have recently been highlighted as potential materials for photovoltaic devices because of their advantages, which include low cost and ease of manufacturing.[1–4] To achieve high performance in conjugated polymer-based solar cells, it is essential to enhance the absorption efficiency of solar energy.[5] Typical conjugated polymers have an energy gap (E_g) of ca. 2.0 eV, can only absorb photons with wavelengths up to ca. 600 nm, and absorb a maximum of 25 % of the total solar energy. By extending the absorption wavelength to 1000 nm (E_g = ~1.2 eV), approximately 70 to 80 % of the solar energy is gained and a notable increase in efficiency can be achieved. Therefore, it is desirable to extend the absorption of the photoactive layer solar cells to wavelengths beyond 600 nm. In addition, charge transport abilities are critical parameters for photovoltaic cells. Higher mobility of the charge carrier in the polymer increases the diffusion lengths of electrons and holes generated during the photovoltaic process and also reduces photocurrent loss by recombination in the active layer, which enhances the charge transfer efficiency from the polymer donor to the [6,6]-phenyl-C_{61}-butyric acid methyl ester acceptor.[6]

Low bandgap polymers are defined as polymers absorbing wavelengths of light longer than 620 nm, corresponding to a band gap below 2.0 eV.[7] There are several factors that influence the bandgap of these polymers, *e.g.*, conjugation length,[8] bond length alternation,[9] resonance energy, dihedral angles,[10] intrachain charge transfer,[11] intermolecular interactions,[12] aromaticity, substituents, etc. The low bandgap polymers presented here are based on two types of electronic structures of benzonoid and quinoid forms and are quite different from polymers containing alternating donor and acceptor segments in the repeating unit.[13] The quinoid form of poly(heteroarylene) is regarded as an excited state of the benzonoid form, and it can be generated by oxidative doping of the benzonoid form. As a result, the quinoid

form of poly(heteroarylene) should have a lower bandgap and, hence, a higher electrical conductivity than the benzonoid form. The higher conductivity of the quinoidal form than that of the benzonoid form is usually observed for the situations of chemical or electrochemical doping for conjugated polymers. It should be noted that electrical conductivity is defined as the product of carrier density and carrier mobility and that the carrier density and carrier mobility are proportional to the bandgap and the delocalisation of the carrier, respectively.

The quinoid form of poly(heteroarylenemethine) consists of benzonoid and quinoid structures in the repeating unit of the main chain (see Scheme 1) and is, therefore, anticipated to have a lower bandgap than the benzonoid form.[14,15] However, the quinoid form of poly(heteroarylenemethine) is unstable due to the nature of the quinoid form itself, which is an excited state of the benzonoid form. Furthermore, the polymer has poor solubility in organic solvents and low processability for the fabrication of devices. Thus, there is a need for the development of novel low bandgap polymers with high stability and solubility in organic solvents.

Here, we focused on poly(bithienylenemethine) and poly(terthienylenemethine) derivatives, where the bithienylene and terthienylene moieties are used as heteroarylenes that increase the effective π-conjugation lengths in the main chain. In addition, terphenylene or terthienylene moieties were introduced as side chains at the methine sites of the main chain (Schemes 1 and 2). The terarylene groups introduced at the methine sites should contribute to delocalisation of π-conjugated electrons over the side chain, leading to stabilisation of the polymer. They should also enhance the solubility of the polymer in organic solvent and help promote polymerisation. In this work, we examined the optical and electrochemical bandgaps of quinoidal polymers with variety of main chains and ternary arylene in side chains.

(Schemes 1 and 2)

Experimental Section

The synthetic routes for the precursor compounds (**1-4)**, side chain molecules (terphenylaldehyde and terthienylaldehyde), and terthiophene are shown in the Supporting Information. **Poly-2PB** was synthesised by a polycondensation reaction between bithiophene and terphenylaldehyde using H_2SO_4. **Poly-2PQ** was prepared by oxidizing **Poly-2PB** with DDQ, followed by washing with organic solvents. The benzonoidal polymers (**Poly-3PB**, **Poly-2TB** and **Poly-3TB**) and the quinoidal polymers (**Poly-3PQ**, **Poly-2TQ** and **Poly-3TQ**) were synthesised in the same manner as **Poly-2PB** and **Poly-2PQ**, respectively.

Synthesis of benzonoidal and quinoidal polymers

Poly-2PB. A mixture of bithiophene (0.25 g, 1.5 mmol), terphenylaldehyde (4″-(pentyloxy)-[1,1′:4′,1″-terphenyl]-4-carbaldehyde) (0.603 g, 1.75 mmol), 4 mL of 1,4-dioxane and 0.05 mL (0.5 mmol) of 96 % sulfuric acid was prepared. The polymerisation temperature was kept constant at 80 °C for 24 h. A dark blue product was precipitated in 500 mL of methanol, redissolved in THF, and then reprecipitated in methanol. Subsequently, the black product was reprecipitated in 500 mL of a mixture of acetone and methanol, redissolved in $CHCl_3$, reprecipitated, filtered in acetone, and dried under vacuum. A dark red polymer was obtained (0.205 g; Yield: 34 %). M_w = 7,400 M_w/M_n = 1.45 (GPC, PS calibration). ^{1}H-NMR ($CDCl_3$, 400MHz, δ from TMS, ppm) δ = 7.59–7.38 (br, 20H, Ph*H*), 6.94 (br, 8H, Th*H*), 6.73 (br, 4H, Ph*H*), 5.76 (br, 1.3H, methine *H*), 3.98 (br, 4H, –OCH_2–),

2.15 (br, 4H, –CH_2–), 1.80 (br, 4H, –CH_2–), 1.44 (br, 4H, –CH_2–), 0.92 (br, 6H, –CH_3). Anal. Calcd for $C_{32}H_{28}OS_2$: C, 78.01 %; H, 5.73 %; O, 3.25 %; S, 13.02 %, Found: C, 76.96 %; H, 5.68 %; O, 4.25 %; S, 13.20 %.

Poly-2PQ. A mixture of 0.1 g of **Poly-2PB**, 0.046 g (0.230 mmol) of DDQ and 1 mL of dry THF was prepared. The reaction temperature was maintained at 60 °C for 24 h. A dark blue product was recovered in 200 mL of stirring methanol, dissolved in THF, and then reprecipitated in methanol. Subsequently, the black product was reprecipitated in 500 mL of a mixture of acetone and methanol, redissolved in $CHCl_3$, reprecipitated, filtered in acetone, and dried under vacuum. A dark red polymer was obtained (0.010 g; Yield: 20 %). ^{1}H NMR ($CDCl_3$, 400MHz, δ from TMS, ppm) δ = 7.6 (br, 12H, Ph*H*), 7.24–7.20 (br, 8H, Th*H*), 6.80–7.00 (br, 12H, Ph*H*), 4.0 (br, 4H, –OCH_2–), 1.90–1.70 (br, 12H, –CH_2–), 0.93 (br, 6H, –CH_3). IR (KBr, cm^{-1}): 2946, 2894 (ν_{CH2}, ν_{CH3}), 1698, 1541 ($\nu_{C=C\ quinoid}$), 1508 ($\nu_{C=C\ benzonoid}$), 818, 799, 720 ($\nu_{C\beta-H}$). Anal. Calcd for $C_{64}H_{54}O_2S_4$: C, 78.17 %; H, 5.53 %; O, 3.25 %; S, 13.02 %, Found: C, 69.11 %; H, 5.09 %; N, 1.07 %; O, 5.45 %; S, 11.34 %.

Poly-3PB. A mixture of terthiophene (0.248 g, 1.0 mmol), terphenylaldehyde (0.400 g, 1.16 mmol), 5 mL of 1,4-dioxane, and 0.02 mL (0.33 mmol) of 96 % sulfuric acid was prepared. The reaction temperature was kept constant at 80 °C for 24 h. A dark blue product was precipitated in 500 mL of methanol, redissolved in THF, and then reprecipitated in methanol. Subsequently, the black product was reprecipitated in 500 mL of a mixture of acetone and methanol, redissolved in $CHCl_3$, reprecipitated, filtered in acetone, and dried under vacuum. A dark red polymer was obtained (0.376 g; Yield: 65.4 %). M_w = 8,000 M_w/M_n = 1.60 (GPC, PS calibration). ^{1}H NMR ($CDCl_3$, 400MHz, δ from TMS, ppm) δ = 7.63 (br, 16H, Ph*H*), 7.43 (br, 4H, Ph*H*), 7.17 (br, 4H, Ph*H*), 6.98 (br, 8H, Th*H*), 6.80 (br, 4H,

Th*H*), 5.80 (br, 1.9H, methine *H*), 4.00 (br, 4H, –OC*H*$_2$–), 2.17 (br, 4H, –C*H*$_2$–), 1.81 (br, 4H, –C*H*$_2$–), 1.42 (br, 4H, –C*H*$_2$–), 0.94 (br, 6H, –C*H*$_3$). Anal. Calcd for $C_{36}H_{30}OS_3$: C, 75.22 %; H, 5.26 %; O, 2.78 %; S, 16.73 %, Found: C, 67.87 %; H, 5.40 %; O, 5.30 %; S, 14.22 %.

Poly-3PQ. A mixture of 0.1 g of **Poly-3PB**, 0.040 g (0.174 mmol) of DDQ, and 2 mL of dry THF was prepared. The reaction temperature was maintained at 60 °C for 24 h. A dark blue product was precipitated in 500 mL of methanol, redissolved in THF, and reprecipitated in methanol. Subsequently, the product was reprecipitated in 500 mL of a mixture of acetone and methanol, redissolved in $CHCl_3$, reprecipitated, filtered in acetone, and dried under vacuum. A dark red polymer was obtained (0.073 g; Yield: 60 %). ^{1}H NMR ($CDCl_3$, 400MHz, δ from TMS, ppm) δ = 7.6 (br, 16H, Ph*H*), 6.97–7.20 (br, 20H, Ph*H* and Th*H*), 3.48 (br, 4H, –OC*H*$_2$–), 1.82 (br, 4H, –C*H*$_2$–), 1.25 (br, 4H, –C*H*$_2$–), 0.91 (br, 14H, –C*H*$_2$– and –C*H*$_3$). IR (KBr, cm^{-1}): 2951, 2854 (ν_{CH2}, ν_{CH3}), 1670, 1599 ($\nu_{C=C\ quinoid}$), 1509 ($\nu_{C=C\ benzonoid}$), 803, 701 ($\nu_{C\beta-H}$). Anal. Calcd for $C_{72}H_{58}O_2S_6$: C, 75.35 %; H, 5.09 %; O, 2.79 %; S, 16.76 %, Found: C, 66.00 %; H, 4.22 %; O, 4.87 %; S, 15.46 %.

Poly-2TB. A mixture of bithiophene (0.026 g, 0.136 mmol), terthienylaldehyde (5″-docosanyl-[2,2′:5′,2″-terthiophene]-5-carbaldehyde) (0.08 g, 0.136 mmol), 0.5 mL of 1,4-dioxane, and 0.024 mL (0.45 mmol) of 96 % sulfuric acid was prepared. The reaction temperature was kept constant at 80 °C for 24 h. A dark blue product was precipitated in 500 mL of methanol, redissolved in THF, and reprecipitated in methanol. Subsequently, the product was reprecipitated in 500 mL of a mixture of acetone and methanol, redissolved in $CHCl_3$, reprecipitated, filtered in acetone, and dried under vacuum. A dark red polymer was obtained (0.077 g; Yield: 71 %). M_w = 2,700 M_w/M_n = 1.17 (GPC, PS calibration). ^{1}H

NMR ($CDCl_3$, 400MHz, δ from TMS, ppm) δ = 7.67 (br, 4H, Th*H*), 7.20 (br, 8H, Th*H*), 6.97 (br, 8H, Th*H*), 5.80 (br, 1.7H, methine *H*), 2.27 (br, 4H, –CH_2–), 1.81–1.24 (br, 80H, –CH_2–), 0.92 (br, 6H, –CH_3).

Poly-2TQ. A mixture of 0.04 g of **Poly-2TB**, 0.012 g (0.055 mmol) of DDQ, and 1 mL of dry THF was prepared. The reaction temperature was maintained at 60 °C for 24 h. A dark blue product was precipitated in 500 mL of methanol, redissolved in THF, and reprecipitated in methanol. Subsequently, the product was reprecipitated in 500 mL of a mixture of acetone and methanol, redissolved in $CHCl_3$, reprecipitated, filtered in acetone, and dried under vacuum. A dark red polymer was obtained (0.013 g; Yield: 30 %). ^{1}H NMR ($CDCl_3$, 400MHz, δ from TMS, ppm) δ = 7.67 (br, 4H, Th*H*), 7.20 (br, 8H, Th*H*), 6.98 (br, 8H, Th*H*), 2.27 (br, 4H, –CH_2–), 1.82–1.25 (br, 80H, –CH_2–), 0.92 (br, 6H, –CH_3). IR (KBr, cm^{-1}): 2963, 2902 (ν_{CH2}, ν_{CH3}), 1682, 1541 ($\nu_{C=C\ quinoid}$), 1508 ($\nu_{C=C\ benzonoid}$), 866, 799, 703 ($\nu_{C\beta\text{-}H}$).

Poly-3TB. A mixture of terthiophene (0.034 g, 0.136 mmol), terthienylaldehyde (0.08 g, 0.136 mmol), 0.5 mL of 1,4-dioxane, and 0.024 mL (0.45 mmol) of 96 % sulfuric acid was prepared. The reaction temperature was kept constant at 80 °C for 24 h. A dark blue product was precipitated in 500 mL of methanol, redissolved in THF, and reprecipitated in methanol. Subsequently, the product was reprecipitated in 500 mL of a mixture of acetone and methanol, redissolved in $CHCl_3$, reprecipitated, filtered in acetone, and dried under vacuum. A dark red polymer was obtained (0.087 g; Yield: 80 %). M_w = 2,800 M_w/M_n = 1.08 (GPC, PS calibration). ^{1}H NMR ($CDCl_3$, 400MHz, δ from TMS, ppm) δ = 7.21 (br, 4H, Th*H*), 7.12–7.04 (br, 16H, Th*H*), 6.95 (br, 4H, Th*H*), 5.97 (br, 1.94H, Th*H*), 2.53 (br, 4H, –CH_2–), 1.62 (br, 4H, –CH_2–), 1.45-1.14 (br, 76H, –CH_2–), 0.92 (br, 6H, –CH_3).

Poly-3TQ. A mixture of 0.051 g of **Poly-3TB**, 0.014 g (0.062 mmol) of DDQ, and 1 mL of dry THF was prepared. The reaction temperature was maintained at 60 °C for 24 h. A dark blue product was precipitated in 500 mL of methanol, redissolved in THF, and reprecipitated in methanol. Subsequently, a black product was reprecipitated in 500 mL of a mixture of acetone and methanol, redissolved in $CHCl_3$, reprecipitated, filtered in acetone, and dried under vacuum. A dark red polymer was obtained (0.03 g; Yield: 60 %). ^{1}H NMR ($CDCl_3$, 400MHz, δ from TMS, ppm) δ = 7.20 (br, 4H, Th*H*), 7.11–7.01 (br, 16H, Th*H*), 6.97 (br, 4H, Th*H*), 2.53 (br, 4H, –C*H*$_2$–), 1.61 (br, 4H, –C*H*$_2$–), 1.47–1.11 (br, 76H, –C*H*$_2$–), 0.92 (br, 6H, –C*H*$_3$). IR (KBr, cm^{-1}): 2959, 2859 (ν_{CH2}, ν_{CH3}), 1684, 1541 ($\nu_{C=C\ quinoid}$), 1508 ($\nu_{C=C\ benzonoid}$), 791, 699 ($\nu_{C\beta-H}$).

Results and Discussion

Synthesis of benzonoidal and quinoidal polymers

We synthesised low bandgap polymers containing alternating benzonoidal and quinoidal structures of thienylene in main chain. The polymers consist of di- or terthienylene moieties with neighboring methine moieties in the main chains. The polymer names are abbreviated as follows: **Poly-** followed by the number of thienylene groups in the main chain (**1** = monothienylene, **2** = bithienylene, and **3** = terthienylene); followed by the side chain group of either terphenylene (**P**) or terthienylene (**T**); followed by either the benzonoidal (**B**) or quinoidal (**Q**) structure of the main chain. Thus, for instance, **Poly-2PQ** is a polymer having bithienylene moiety in the main chain, a terphenylene moiety in the side chain, and showing a quinoidal structure. The alkyl groups at the terminal sites of the terphenylene and terthienylene side chains are pentyloxy (-OC_5H_{11}) and docosyl (-$C_{22}H_{45}$) groups, respectively. It should be noted that the terthienylene moiety is more rigid in terms of internal rotation.

Hence, it is more planar than the terphenylene moiety, and the polymer bearing terthienylene in the side chains would be less soluble in organic solvents than the polymer bearing terphenylene. Thus, to improve the low solubility resulting from terthienylene side chains, we used a docosyl group ($-C_{22}H_{45}$) as the terminal group at the terthienylene side chains, which is a longer alkyl group compared to the pentyloxy group ($-OC_5H_{11}$) used on the terphenylene side chains.

As a preliminary experiment, we synthesised monothienylene-based polymers with terphenylene (**Poly-1PB**, **-1PQ**) or terthienylene side chains, (**Poly-1TB**, **-1TQ)** (Scheme S2 in the supporting information). We also synthesised hexyl-substituted monothienylene (**Poly-1HTB**, **-1HTQ**) and bithienylene **(Poly-2HTB**, **-2HTQ**)-based polymers with terthienylene side chains (Scheme S4). However, these polymers showed low degrees of polymerisation, resulting in fragile films (Table S2).

In contrast, the benzonoidal bithienylene polymer with terphenylene side chains (**Poly-2PB**) had a lower degree of dispersion in molecular weight and was obtained in higher yield compared to those with phenylene and biphenylene moieties in side chains (Table S1). This result was attributed to the larger stabilisation effect of the terphenylene moiety contributing more effectively to the delocalisation of π-electrons of the main chain over the side chain compared to the phenylene and biphenylene moieties. The methine site located between the benzonoid and quinoid moieties in the main chain is regarded as a defect point at which π-conjugation of the main chain is suppressed if the methine site is substituted with an alkyl group. However, when an aryl group such as a phenylene or thienylene moiety is substituted at the methine site, π-conjugation can be significantly stabilised due to a through space interaction of π-electrons between the main and side chains. Therefore, we used the terphenylene or terthienylene moieties as side chains of the present polymer. In addition,

alkyl groups were introduced to the terminal sites of the terarylene to increase the solubility of the polymers in organic solvents.

The benzonoidal polymers (**Poly-2PB**, **Poly-3PB**, **Poly-2TB** and **Poly-3TB)** were synthesised by polycondensation reactions using concentrated sulfuric acid (H_2SO_4). The quinoidal polymers (**Poly-2PQ**, **Poly-3PQ**, **Poly-2TQ** and **Poly-3TQ**) were prepared by oxidative dehydrogenations of the corresponding benzonoidal polymers using 2,3-dichloro-5,6-dicyano-1,4-benzoquinone (DDQ) (see Schemes 1 and 2). Details on the synthesis of the monomers and polymers are provided in the Supporting Information.

All polymers were purified by precipitation using methanol and a mixed solvent (methanol/acetone/$CHCl_3$). Generation of the alternating benzonoid and quinoid structure in the polymers was confirmed from NMR measurements. Figure 1 shows ^{1}H NMR spectra of **Poly-2PB** and **Poly-2PQ** in CD_3Cl. The peak at 5.8 ppm assigned to the methine group of **Poly-2PB** disappeared when the polymer was oxidised with DDQ. The integration value of the methine peak of **Poly-2PB** was 1.3 H, indicating that **Poly-2PB** consisted of 65 % of the benzonoidal structure and 35 % of the quinoidal structure in the repeating unit. This result indicates that the methine moieties in **Poly-2PB** were partially oxidised during the polymerisation by the sulfuric acid.

(Figure 1)

The molecular weights of the polymers were determined by gel permeation chromatography (GPC) in THF using a polystyrene standard. The polymerisation results are shown in Table 1. The degrees of polymerisation in **Poly-2PQ** and **Poly-3PQ** were 10 and 9, respectively, which implies that the numbers of the thienylene units in **Poly-2PQ** and

Poly-3PQ were 20 and 27, respectively. Meanwhile, the degrees of polymerisation in **Poly-2TQ** and **Poly-3TQ** were 3 and 3, respectively, implying that the numbers of the thienylene unit in **Poly-2TQ** and **Poly-3TQ** were 6 and 9, respectively. It is clear that the molecular weights and degrees of polymerisation of **Poly-2PB** and **Poly-3PB** were larger than those of **Poly-2TB** and **Poly-3TB**. This difference suggests that the terphenylene moiety is more favourable as a side chain in the arylene methine-based polymer than the terthienylene moiety.

(Table 1)

We investigated thermal stability of the quinoidal polymers. Figure 2 depicts thermogravimetry (TG) data. It is seen that although **Poly-2PQ** and **Poly-3PQ** are gradually decomposed upon heating, **Poly-2TQ** and **Poly-3TQ** show a drastic degradation at approximate 350 °C. Thus, the former polymers (**Poly-2PQ**, **Poly-3PQ**) are thermally more stable than the latter polymers (**Poly-2TQ**, **Poly-3TQ**). This difference is mainly due to the difference of molecular weights. Namely, the degrees of polymerisation of the corresponding precursors of the former (**Poly-2PB** and **Poly-3PB**) are approximate three times higher than those of the latter (**Poly-2TB** and **Poly-3TB**), as shown in Table1. These results suggest that the quinoidal polymers with terphenylene moieties have good thermal stability and suitable for annealing process.

Subsequently, we examined the polymer structures of the quinoidal polymers. Figure 3 depicts powder X-ray diffraction (XRD) patterns of the polymers. Broad and weak diffractions at approximate 12.7~18.0 Å were observed in small angle region (2θ = 4.9~7.0°). These diffractions may correspond to the distances between next-neighbouring side chains

that are located in the same sites among alternatively positioning side chains (see Figure 3). Meanwhile, the broad diffractions at approximate 4 Å were observed in wide angle region (2θ = 18.9~**22**.0°), corresponding to the distances between π–stacked polymers chains. It is likely that the polymers (**Poly-2TQ** and **Poly-3TQ**) with terthienylene side chains are closer π–stacked than those (**Poly-2PQ** and **Poly-3PQ**) with terphenylene side chains due to a more planar structure of the terthienylene side chains.

(Figure 2 and 3)

The quinoidal polymers were investigated by various spectroscopic methods after the oxidative dehydrogenations of benzonoidal polymers by DDQ. The results from NMR, GPC, and infrared (IR) spectra verified the proposed benzonoidal and quinoidal structures of the prepared polymers (Figure S1).

Optical properties

Figure 4 shows the UV-Vis-NIR absorption spectra of the benzonoidal and quinoidal polymers in $CHCl_3$ ($c = 1 \times 10^{-4}$ M). **Poly-2PQ** exhibited a broad band at 600 nm due to a π-π* transition of the main chain with a quinoidal structure. A very weak band at 600 nm was also observed in **Poly-2PB** due to its partial oxidation by sulfuric acid during the polycondensation. The band at approximate 300 nm was attributed to the terphenylene moiety in the side chain. **Poly-2PQ** also showed a broad band from 900 nm to the NIR region.

(Figure 4)

Poly-3PQ showed a shoulder at 750 nm and a broad band at 970 nm, which are 150 nm and 370 nm longer, respectively, than the corresponding band of **Poly-2PQ** at 600 nm. This red shift is due to an increase in the effective conjugation length in **Poly-3PQ**. In addition, **Poly-3PQ** showed intense bands for the side chains and the quinoidal segments of the main chain at ca. 300 nm and 400 nm, respectively. The optical bandgaps were evaluated from the absorption edges of the polymers. Interestingly, the quinoidal polymers exhibited absorption bands with long tails up to the NIR region, which made it difficult to strictly determine the onset of the absorption bands. Nevertheless, the optical bandgaps of **Poly-2PQ** and **Poly-3PQ** were estimated to be 1.7 eV and 0.8 eV, respectively.

Poly-2TQ and **Poly-3TQ**, which had terthienylene moieties in their side chains, showed absorption spectra similar to **Poly-2PQ** and **Poly-3PQ**, respectively. As seen in Figure 4c and 4d, **Poly-2TQ** and **Poly-3TQ** exhibited absorption bands at 700 nm and 890 nm, respectively, due to a π-π^* transition of the main chain with a quinoidal structure. The optical bandgaps of **Poly-2TQ** and **Poly-3TQ** were estimated to be 1.5 eV and 0.8 eV, respectively. Although **Poly-2TQ** showed no band in the NIR region, **Poly-3TQ** showed a broad band in the range from the visible to the NIR region due to the quinoidal structure.

Changing from the terphenylene moiety to the terthienylene in the side chains caused a slight decrease in the optical bandgap between **Poly-2PQ** and **Poly-2TQ**, possibly due to the higher planarity of the terthienylene moiety. However, the planarity of the terthienylene moiety reduced the flexibility and solubility of the polymers. This is the reason why a much longer alkyl chain, i.e., a docosyl group ($-C_{22}H_{45}$), at the terminal site of the terthienylene in the side chains was used to improve the solubility of the polymer. Nevertheless, the

intrinsically lower solubility of the polymers bearing terthienylene side chains caused premature termination of the polymerisation, resulting in low molecular weights for **Poly-2TQ** and **Poly-3TQ**, although these polymers exhibited lower bandgaps based on optically evaluation (see Table 2).

Electrochemical properties

Figure 5 shows cyclic voltammetry (CV) results for quinoidal polymer films. The films were prepared by spin-casting the polymer solutions (5 mg/mL in $CHCl_3$) onto ITO glasses (10 mm × 30 mm × 1 mm, 10 Ω/cm^2). Note that **Poly-2TQ** and **Poly-3TQ** showed low uniformity and brittleness in the spin-cast films because of their poor solubility in organic solvents and low molecular weights (see Table 1).

(Figure 5)

The CV curves of polymer films were recorded with a voltage of 10 mV/s in 0.1 M tetrabutylammonium perchlorate (TBAP)/acetonitrile. Ag/AgCl was used as a reference electrode and calibrated with ferrocene. The half-wave potential of the ferrocene/ferrocenium (Fc/Fc^+) redox couple [$E_{1/2}$ (Fc/Fc^+ vs. Ag/AgCl)] was estimated from the following equation:

$$E_{1/2}\,(Fc/Fc^+ \text{ vs. } Ag/AgCl) = (E_{ap} + E_{cp})/2\,, \quad (1)$$

where, E_{ap} and E_{cp} are the anodic and cathodic peak potentials, respectively. The half-wave potential of Fc/Fc^+ was found to be 0.52 V relative to the Ag/Ag^+ reference electrode. A

method for evaluating HOMO and LUMO energy levels using the onset potentials, $E_{ox/onset}$ and $E_{red/onset}$, has previously been reported.[16] This conventional method was used here to estimate the HOMO and LUMO energy levels of polymers on the basis of the reference energy level of ferrocene (4.8 eV below the vacuum level) as follows:

$$E_{HOMO} = -[4.8\ eV - E_{1/2}\ (Fc/Fc^{+}\ vs.\ Ag/AgCl) + E_{ox/onset}\ (vs.\ Ag/AgCl)], \quad (2)$$

$$E_{LUMO} = -[4.8\ eV - E_{1/2}\ (Fc/Fc^{+}\ vs.\ Ag/AgCl) + E_{red/onset}\ (vs.\ Ag/AgCl)]. \quad (3)$$

The oxidation and reduction potentials ($E_{ox/potential}$ and $E_{red/potential}$) of **Poly-2PQ** were +1.63 V and −1.23 V, respectively, and those of **Poly-3PQ** were +0.74 V and −1.67 V, respectively. The $E_{ox/onset}$ and $E_{red/onset}$ of **Poly-2PQ** were +1.37 V and −0.80 V, respectively, and those of **Poly-3PQ** were +0.39 V and −1.22 V, respectively. Thus, the E_{HOMO} and E_{LUMO} of **Poly-2PQ** were estimated to be −5.7 eV and −3.5 eV, respectively, and those of **Poly-3PQ** were estimated to be −4.7 eV and −3.1 eV, respectively (Table 2, Figure 5a and b). The E_{HOMO} and E_{LUMO} of **Poly-3PQ** were higher than those of **Poly-2PQ**, respectively, owing to an increase in the effective conjugation length of the main chain of **Poly-3PQ**. The electrochemical bandgaps estimated from the E_{HOMO} and E_{LUMO} of **Poly-2PQ** and **Poly-3PQ** were 2.2 eV and 1.6 eV, respectively.[17]

Figure 5c and d show cyclic voltammograms (CV) of the quinoidal polymers with terthienylene moiety in side chain (**Poly-2TQ** and **Poly-3TQ**) in redox process. The E_{HOMO} and E_{LUMO} of **Poly-2TQ** were estimated to be −4.7 eV and −3.0 eV, and those of **Poly-3TQ** were estimated to be −4.5 eV and −3.3 eV respectively. The electrochemical bandgaps estimated from the E_{HOMO} and E_{LUMO} of **Poly-2TQ** and **Poly-3TQ** were 1.7 and 1.2 eV,

respectively. The optical and electrochemical bandgaps of present polymers (**Poly-2PQ**, **Poly-3PQ Poly-2TQ**, and **Poly-3TQ**) are summarised in Table 2. It is of interest that the bandgaps of the present polymers are comparable to or smaller than that of poly(3-hexylthiophene) (**P3HT**; 1.9 eV). The electrochemical bandgaps of the polymers were larger than the optical bandgaps due to extra energy requirements for redox potentials as well as the interface barrier for charge injection.[18–20] The difference between the electrochemical bandgap and the optical bandgap gives the electron-hole Coulomb interaction energy.

(Table 2)

Figure 6 shows the results of molecular mechanics (MM) calculations[21] depicting three-dimensional models of the benzonoidal polymer **Poly-2PB** and quinoidal polymer **Poly-2PQ**. In **Poly-2PB**, the main chain has a less planar and zigzag structure, and the side chains extend randomly from the main chain. In **Poly-2PQ**, however, the main chain shows a planar and straight but slightly curved structure, and the side chains are orthogonal to the main chain. These results suggest that the quinoidal polymer has a longer effective conjugation length to result in a smaller bandgap compared to the benzonoidal polymer. This result is in agreement with the experimental results mentioned above.

(Figure 6)

Hole mobility and electrical conductivity of quinoidal polymers

Finally, it may be worthwhile to discuss the energy levels of the present polymers and the related materials from the viewpoint of charge carrier mobility in the photovoltaic cell. The

charge carrier mobility in blend films can be evaluated by the space charge limited current (SCLC) method, for which the hole-only device with the same active layer thickness as actual devices is fabricated by constructing ITO / **PEDOT–PSS** / active polymer–**PCBM** (1:1) / aluminium structure (Figure S6). Here, ITO is indium tinoxide, **PEDOT** is poly(3,4-ethylenedioxythiophene), **PSS** is poly(styrenesulfonic acid), and **PCBM** is [6,6]-phenyl-C_{61}-butyric acid methyl ester. **PEDOT**–**PSS** is used as a hole-conducting buffer. The solar cell containing the active layer of **Poly-2PQ**–**PCBM** exhibited a hole mobility of 3.4×10^{-5} $cm^2 V^{-1} s^{-1}$, which is one order lower than that of the solar cell containing **P3HT**–**PCBM** (3.0×10^{-4} $cm^2 V^{-1} s^{-1}$). This may be due to the low molecular weight of **Poly-2PQ**. The hole mobility could be improved by increasing the effective conjugation length of the polymer which should enhance delocalization of the charge carrier such as hole. Note that the hole mobilities of other type of the quinoidal polymers were not able to be measured due to their poor film fabrication and also their low molecular weights.

The electrical conductivities of the polymer films were evaluated by measuring the surface resistance.[22] The surface resistance and electrical conductivities of the quinoidal polymer films before and after iodine (I_2)-doping are shown in Table 3. The **Poly-2PQ** film showed a conductivity of 9.5×10^{-7} S/cm. The I_2-doped **Poly-2PQ** film showed an increase in conductivity by more than one order, i.e., 2.0×10^{-5} S/cm. The effect of I_2 doping in increasing the conductivity is confirmed in **Poly-2PQ**. However, the conductivity of the present quinoidal polymer still remains semiconducting even after the doping. Thus it is required to lengthen the effective conjugation length of the polymer.

(Table 3)

Energy levels of the quinoidal polymers

In Figure 7 are depicted the HOMO and LUMO levels of the present quinoidal polymers and **PEDOT-PSS** and **PCBM**, as well as the energy levels of ITO and aluminium. For comparison, the HOMO and LUMO levels of **P3HT** with M_n = 18,000 are also shown in this figure.

(Figure 7)

The LUMO levels of the present quinoidal polymers (–3.0 ~ –3.5 eV for **Poly-2PQ, Poy-3PQ, Poly-2TQ,** and **Poly-3TQ**) are higher than that of **PCBM** (–4.1 eV; an electron acceptor), which should promote the transfer of electrons generated by charge separation to **PCBM**. Meanwhile, the HOMO levels of the polymers (–4.7 ~ –4.5 eV for **Poly-3PQ**, **Poly-2TQ**, **Poly-3TQ**) are very close to that of ITO (–4.7 eV). Thus, transfer of the hole generated by charge separation from the polymer to ITO through **PEDOT-PSS** is easy to occur, although reverse transfer of the hole from ITO to the polymer may also occur.

It is of interest to note that the LUMO levels of the quinoidal polymers, particularly that of **Poly-2PQ** (–3.5 eV), are closer to that of **PCBM** (–4.1 eV) than **P3HT** (–2.9 eV). Thus, electrons generated by charge separation in the **Poly-2PQ-PCBM** system transfer more easily to the aluminium through **PCBM** compared to the **P3HT-PCBM** system. However, the HOMO level of **Poly-2PQ** (–5.7 eV) is more largely separated from that of the ITO (–4.7 eV) anode compared to **P3HT** (–4.8 eV). Therefore, it may be more difficult for the hole generated by the charge separation to transfer from **Poly-2PQ** to ITO compared to the case of

P3HT. It is anticipated that the more difficult hole transfer from **Poly-2PQ** to ITO may be improved by using **PEDOT-PSS** as a hole-conducting buffer, because the HOMO level of **PEDOT-PSS** (−5.2 ~ −5.3 eV)[23] is between that of **Poly-2PQ** and ITO.

Conclusion

New types of low bandgap polymers, poly(bithienylenemethine) and poly(terthienylenemethine) derivatives, containing alternating benzonoidal and quinoidal structures in the main chains, were synthesised by introducing arylene moieties in the side chains. The bandgaps of these polymers were tuned by changing the repeating units of the main chain and by achieving oxidative dehydrogenation of the benzonoidal polymers. The terphenylene or terthienylene moieties on the side chains helped stabilize the quinoidal structure of the main chain by delocalizing the π-electrons of the main chain over the side chain. The quinoidal polymers exhibited small optical and electrochemical bandgaps, as expected. Namely, the optical and electrochemical bandgaps of the bithienylene-based quinoidal polymer with the terphenylene side chain (**Poly-2PQ**) were 1.7 and 2.2 eV, respectively, and those of the terthienylene-based quinoidal polymer with the terphenylene side chain (**Poly-3PQ**) were 0.8 and 1.6 eV, respectively. Similarly, those of bithienylene-based quinoidal polymer with the terthienylene side chain (**Poly-2TQ**) were 1.5 and 1.7 eV, respectively, and those of the terthienylene-based quinoidal polymer with terthienylene side chain (**Poly-3TQ**) were 0.8 and 1.2 eV, respectively. In addition, the quinoidal polymers with the terphenylene moieties in the side chains (**Poly-2PQ** and **Poly-3PQ**) were easily

formed into films, but those with the terthienylene moieties in the side chains (**Poly-2TQ** and **Poly-3TQ**) exhibited poor film formation owing to their low molecular weight.[24] The present quinoidal polymers bearing terphenylene moieties in the side chains could be potential materials for plastic electronics.

Acknowledgements

The authors are grateful to Mr. Ryousuke Shimizuguchi and Mr. Yasuyuki Imamura (Kyoto University) for their helpful cooperation in synthesizing monomers and polymers. The authors thank Dr. T. Asano, Dr. S. Hayashi, and Dr. T. Okabe (JX Nippon Oil & Energy Corporation) for the measurements of the hole mobilities, and Mr. K. Sakai for measurement of electrical conductivity (Mitsubishi Chemical Analytech). This work was supported by Grant-in-Aids for Science Research (A) (No. 25246002) and (No. 25620098) from the Ministry of Education, Culture, Sports, Science and Technology, Japan.

References

1. (a) G. Yu, J. Gao, J. C. Hummelen, F. Wudl, A. J. Heeger, *Science*, 1995, **270**, 1789–1891. (b) C. J. Barbec, N. S. Sariciftci, J. C. Hummelene, *Adv. Funct. Mater.*, 2001, **11**, 15–26. (c) S. Günes, H. Neugebauer, N. S. Sariciftci, *Chem. Rev.*, 2007, **107**, 1324–1338. (d) F. C. Krebs, *Sol. Energ. Mat. Sol. Cells*, 2009, **93**, 394–412.

2. (a) *Handbook of Conjugated Polymers: Theory, Synthesis, Properties, and Characterisation,* ed. T. A. Skotheim and J. R. Reynolds, CRC Press, New York, 2nd edn., 2006. (b) *Third Generation Photovoltaics: Advanced Solar Energy Conversion*, ed. M. A.

Green, Springer, New York, 2006. (c) *Polymer Photovoltaics: A Practical Approach*, ed. F. C. Krebs, SPIE Press. 2008. (d) *Organic Solar Cells: Materials and Device Physics*, ed. C. H. C. Wallace, Springer, New York, 2013.

3. (a) B. Oregan, M. Gratzel, *Nature*, 1991, **353**, 737–740. (b) M. Law, L. E. Greene, J. C. Johnson, *Nat. Mater*., 2005, **4**, 455–459. (c) N. Robertson, *Angew. Chem. Int. Ed*., 2006, **45**, 2338–2345. (d) A. Hagfeldt, G. Boschloo, LC Sun, L. Kloo, H. Pettersson, *Chem. Rev*., 2010, **110**, 6595–6663. (e) Y. J. Cheng, S. H. Yang, C. S. Hsu, *Chem. Rev*., 2009, **109**, 5868–5923.

4. (a) R. H. Friend, *Nature*, 1995, **376,** 498–500. (b) A. J. Heeger, *Science,* 1995, **2 70**, 1789–1791. (c) G. Dennler, M. C. Scharber, C. J. Brabec, *Adv. Mater*., 2009, **21**, 1 323–1338.

5. (a) M. C. Scharber, D. Mühlbacher, M. Koppe, P. Denk, C. Waldauf, A. J. Heeger, C. J. Brabec, *Adv. Mater*., 2006, **18**, 789–794. (b) J. Y. Kim, K. H. Lee, N. E. Coates, D. Moses, T. Q. Nguyen, M. Dante, A. J. Heeger, *Science*, 2007, **317**, 222–225.

6. G. Li, V. Shirotriya, J. Huang, Y. Yao, T. Moriarty, K. Emery, Y. Yang, *Nat. Mater.,* 2005, **4**, 864–868.

7. (a) S. E. Shaheen, G. E. Jabbour, M. M. Morrell, Y. Kawabe, B. Kippelen, N. Peyghambarian, M.-F. Nabor, R. Schlaf, E. A. Mash, N. R. Armstrong, *J. Appl. Phys.*, 1998, **84**, 2324–2327. (b) Y. S. Jeong, K. Akagi, *J. Mater. Chem*., 2011, **21**, 10472–10481. (c) Y. S. Jeong, K. Akagi, *Macromolecules*, 2011, **44**, 2418–2426. (d) K. Akagi, *Chem. Rev*., 2009, **109***,* 5354–5401.

8. (a) J. L. Brédas, A. J. Heeger, F. Wudl, *J. Chem. Phys*., 1986, **85**, 4673–4678. (b) M. Kobayashi, N. Colaneri, M. Boysel, F. Wudl, A. J. Heeger, *J. Chem. Phys.,* 1985, **82**,

5717–5723.

9. (a) S. R. Marder, C. B. Gorman, B. G. Tiemann, J. W. Perry, G. Bourhill, K. Mansour, *Science*, 1993, **261**, 186–189. (b) J. M. Hales, J. Matichak, S. Barlow, S. Ohira, K. Yesudas, J. L. Brédas, J. W. Perry, S. R. Marder, *Science*, 2010, **327**, 1485–1488.

10. P. M. Viruela, R. Viruela, E. Oriti, J. L. Brédas, *J. Am. Chem. Soc*., 1997, **119,** 1360–1369.

11. (a) J. L. Brédas, D. Beljonne, V. Coropceanu, J. Cornil, *Chem. Rev*., 2004, **10**, 4971–5003. (b) E. Bundgaard, F. C. Krebs, *Sol. Energ. Mat. Sol. Cells,* 2007, **91**, 954–985. (c) S. A. Jenekhe, L. Lu, M. M. Alam, *Macromolecules*, 2001, **34**, 7315–7324.

12. Y. Kim, S. Cook, S. M. Tuladhar, S. A. Choulis, J. Nelson, J. R. Durrant, D. D. C. Bradley, M. Giles, I. Mcculloch, C. S. Ha, M. Ree, *Nat. Mater.*, 2006, ***5***, 197–203.

13. (a) M. Catellani, S. Luzzati, N.-O. Lupsac, R. Mendichi, R. Consonni, A. Famulari, S.V. Meille, F. Giacalone, J. L. Segura, N. Martin, *J. Mater. Chem.,* 2004, **14**, 67–74. (b) E. E. Sheina, S. M. Khersonsky, E. G. Jones, R. D. McCullough, *Chem. Mater.,* 2005, **17**, 3317–3319.

14. (a) W. C. Chen, S. A. Jenekhe, *Macromolecules*, 1995, **28**, 454–464. (b) W. C. Chen, S. A. Jenekhe, *Macromolecules*, 1995, **28,** 465–480. (c) W. C. Chen, C. L. Liu, C. T. Yen, F. C. Tsai, C. J. Tonzola, N. Olson, S. A. Jenekhe, *Macromolecules*, 2004, **37**, 5959–5964.

15. (a) H. Goto, K. Akagi, H. Shirakawa, *Synt. Met*., 1997, **84**, 385–386. (b) K. Akagi, H. Goto, M. Okuda, H. Shirakawa, *Mol. Cryst. Liq. Cryst*., 1998, **316**, 201–204. (c) R. H. Kiebooms, H. Goto, K. Akagi, *Macromolecules*, 2001, **34**, 7989–7998. (d) H. Goto, K. Akagi, *J. Polym. Sci. Part A: Polym. Chem.,* 2005, **43**, 619–629.

16. *Electrochemical Methods: Fundamentals and Applications,* ed. A. J. Bard and L. R. Fraulkner, Wiley & Sons, Inc., New York, 2nd edn., 2001.

17. The HOMO and LUMO levels of monothienylene-based polymer with terphenylene (**Poly-1PQ**) were estimated to be –6.5 eV and –3.0 eV, respectively. The electrochemical bandgap of **Poly-1PQ** was 3.5 eV (see Figure S3).

18. (a) Z. K. Chen, W. Huang, L. H. Wang, E. T. Kang, B. J. Chen, C. S. Lee, S. T. Lee, *Macromolecules*, 2000, **33**, 9015–9020. (b) S. Janietz, D. D. C. Bradley, M. Grell, C. Giebeler, M. Inbasekaran, E. P. Woo, *Appl. Phys. Lett.*, 1998, **73**, 2453–2455.

19. (a) Y. F. Li, Y. P. Zou, *Adv. Mater.*, 2008, **20**, 2952–2958. (b) L. Dunsch, P. Rapta, N. Schulte, A. D. Schlüter, *Angew. Chem. Int. Ed.,* 2002, **41**, 2082–2085.

20. R. J. Kline, M. D. McGehee, M. F. Toney, *Nat. Mater.*, 2006, **5**, 222–228.

21. Energetically optimised conformations of benzonoidal and quinoidal polymers were obtained by molecular mechanics (MM) calculations using the MMFF94 force field program (Wavefunction, Inc., Spartan 10).

22. T. C. Huang, H. E. Yin, W. Y. Chiu, C. F. Lee, *Thin Solid Films*, 2014, **552**, 98–104.

23. (a) Z. Wang, J. Qi, X. Yan, Q. Zhang, Q. Wang, S. Lu, P. Lin, Q. Liao, Z. Zhang, Y. Zhang, *RSC Adv.*, 2013, **3**, 17011–17015. (b) Y. Zhang, L. Ge, M. Yan, S. Ge, J. Yu, X. Song, B. Gao, *Chem.Comm.*, 2014, **50**, 1417–1419.

24. We tried to increase the molecular weights of the polymers by using another acidic catalysts such as such as methane sulphonic acid, *p*-toluene sulphonic acid, 4-ethylenebenzene sulphonic acid and also by refining the polymerization conditions, especially polymerization time. These results are shown in Scheme S5 and Table S3. The polymerization results indicated substantial increases in molecular weight of the benzonoidal polymers when alkyl and aromatic sulfonic acids are used. Actually, the degree of

polymerization for **Poly-2PB** was in the range from 8 to 17, which was comparable to or approximate two times higher than the value (D.P. = 10) of the polymer synthesized by sulfuric acid. The details of the polymers synthesized by alkyl and aromatic sulfonic acids will be reported elsewhere.

Captions of Schemes, Figures, and Tables

Scheme 1. Synthetic routes for benzonoidal and quinoidal polymers with ternary phenylene or thienylene moieties in side chains.

Scheme 2. Structures of benzonoidal (**Poly-2PB**, **Poly-3PB**, **Poly-2TB**, **Poly-3TB**) and quinoidal (**Poly-2PQ**, **Poly-3PQ**, **Poly-2TQ**, **Poly-3TQ**) polymers with ternary phenylene or thienylene moieties in their side chains.

Figure 1. ^{1}H-NMR spectra of **Poly-2PB** (blue line) and **Poly-2PQ** (red line) in $CDCl_3$. The methine proton signal at ca. 5.8 ppm is indicated with a green dotted line box.

Figure 2. TG plots of quinoidal polymers (**Poly-2PQ**, **Poly-3PQ**, **Poly-2TQ**, and **Poly-3TQ**) with heating rate of 10 °C/min in N_2.

Figure 3. (upper) X-ray diffraction patterns of (a) **Poly-2PQ**, (b) **Poly-3PQ**, (c) **Poly-2TQ**, and (d) **Poly-3TQ**. (lower) Schematic representation of quinoidal polymer. The distances between the next-neigbouring site chains were evaluated by molecular mechanics calculations using MMFF94 force field program (Spartan 10), where the quinoidal polymers with 10 repeating units consisting of alternative benzonoidal and quinoidal moieties were employed as model systems.

Figure 4. UV-Vis-NIR absorption spectra of (a) **Poly-2PB** and **Poly-2PQ**, (b) **Poly-3PB** and **Poly-3PQ**, (c) **Poly-2TB** and **Poly-2TQ** and (d) **Poly-3TB** and **Poly-3TQ** in $CHCl_3$. The blue and red lines in the spectra indicate the benzonoidal and quinoidal polymers, respectively.

Figure 5. Cyclic voltammograms of (a) **Poly-2PQ** and (b) **Poly-3PQ**, (c) **Poly-2TQ**, and (d) **Poly-3TQ** films on a platinum electrode in acetonitrile containing 0.1 M tetrabutylammonium perchlorate (TBAP) measured with a scan rate of 10 mV/sec.

Figure 6. Three-dimensional models for the benzonoidal polymer, **Poly-2PB** (above) and the quinoidal polymer, **Poly-2PQ** (below).

Figure 7. (a) Comparison of energy levels between **P3HT**, quinoidal polymers, and **PCBM**. (*): HOMO and LUMO levels of the quinoidal polymers were measured from cyclic voltammograms. (b) The molecular structure of **PEDOT-PSS** and **PCBM**, and polymer structures of **P3HT**, **Poly-2PQ**, **Poly-3PQ**, **Poly-2TQ**, and **Poly-3TQ**.

Table 1. Polymerisation results of **Poly-2PB**, **Poly-3PB**, **Poly-2TB** and **Poly-3TB**.

a) D.P.: Degree of polymerisation

b) T.U.: Number of thienylene unit

Table 2. Optical and electrochemical bandgaps of **Poly-2PQ**, **Poly-3PQ**, **Poly-2TQ** and **Poly-3TQ**.

a) Reduction and oxidation potentials measured by cyclic voltammetry.

b) The reduction and oxidation potentials were evaluated assuming that the absolute energy level of ferrocene/ferrocenium is below 4.8 eV in a vacuum.

Table 3. Surface resistance and electrical conductivity of quinoidal polymer films

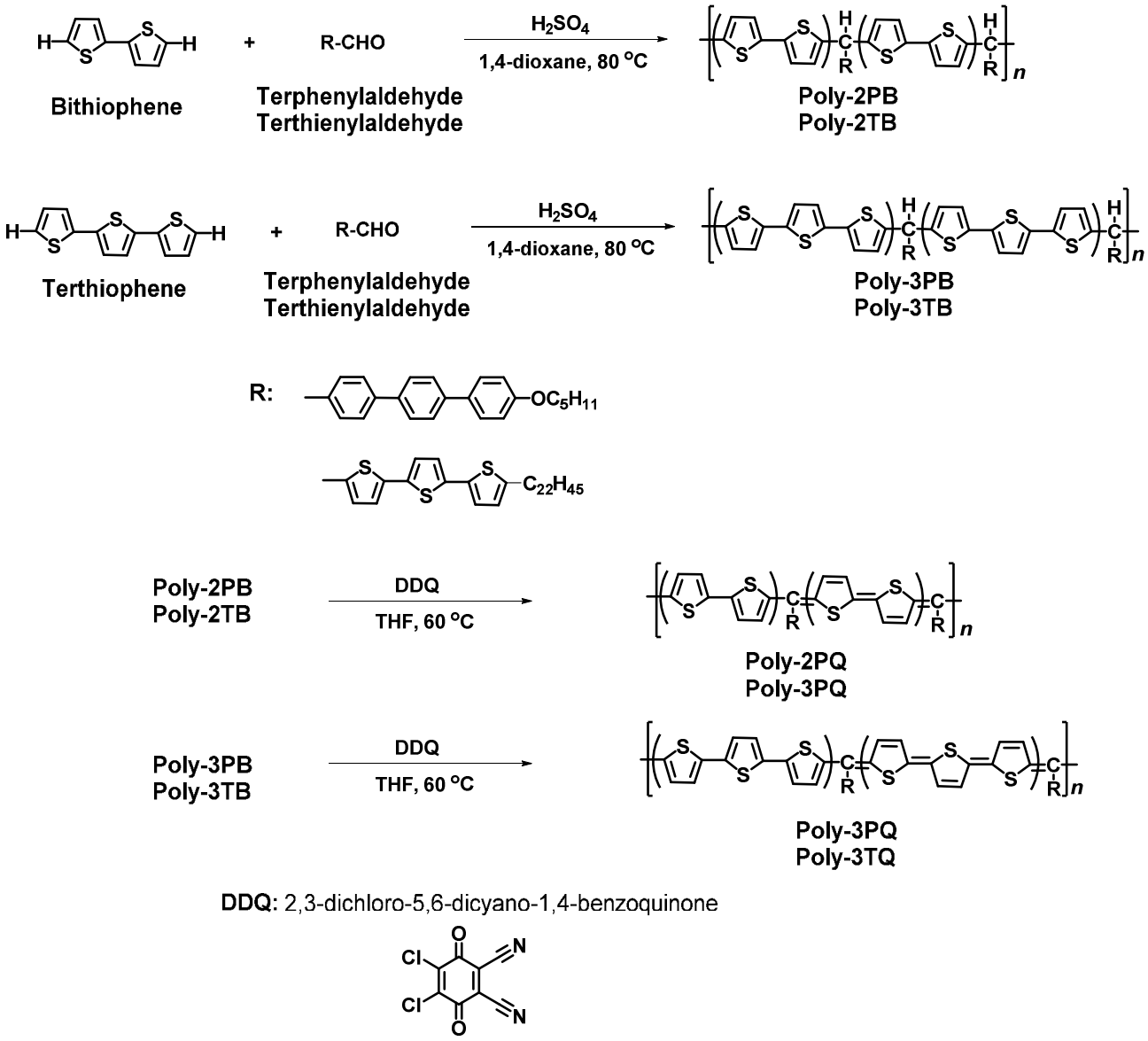

DDQ: 2,3-dichloro-5,6-dicyano-1,4-benzoquinone

Scheme 1. Synthetic routes for benzonoidal and quinoidal polymers with ternary phenylene or thienylene moieties in side chains.

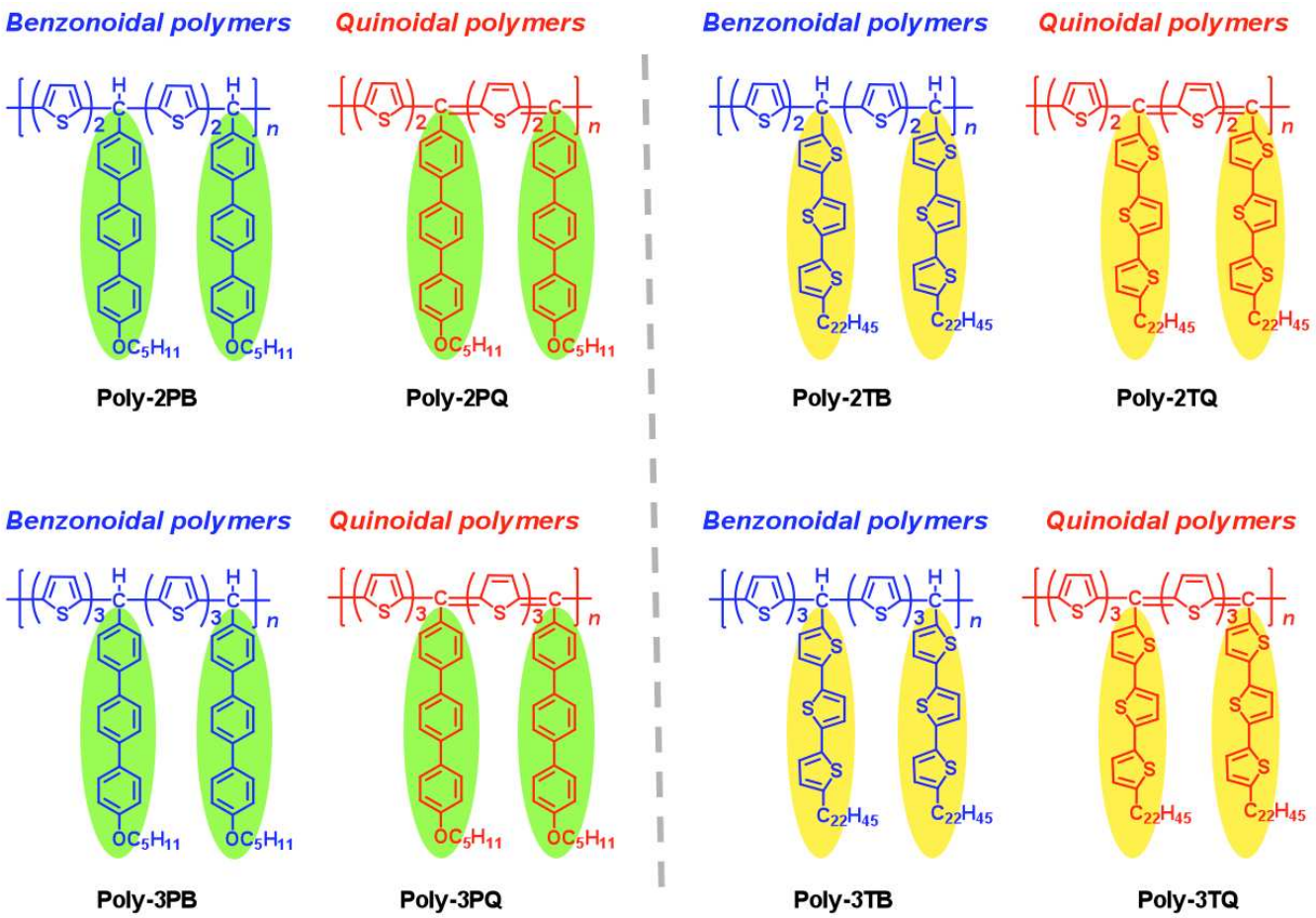

Scheme 2. Structures of benzonoidal (**Poly-2PB**, **Poly-3PB**, **Poly-2TB**, **Poly-3TB**) and quinoidal (**Poly-2PQ**, **Poly-3PQ**, **Poly-2TQ**, **Poly-3TQ**) polymers with ternary phenylene or thienylene moieties in their side chains.

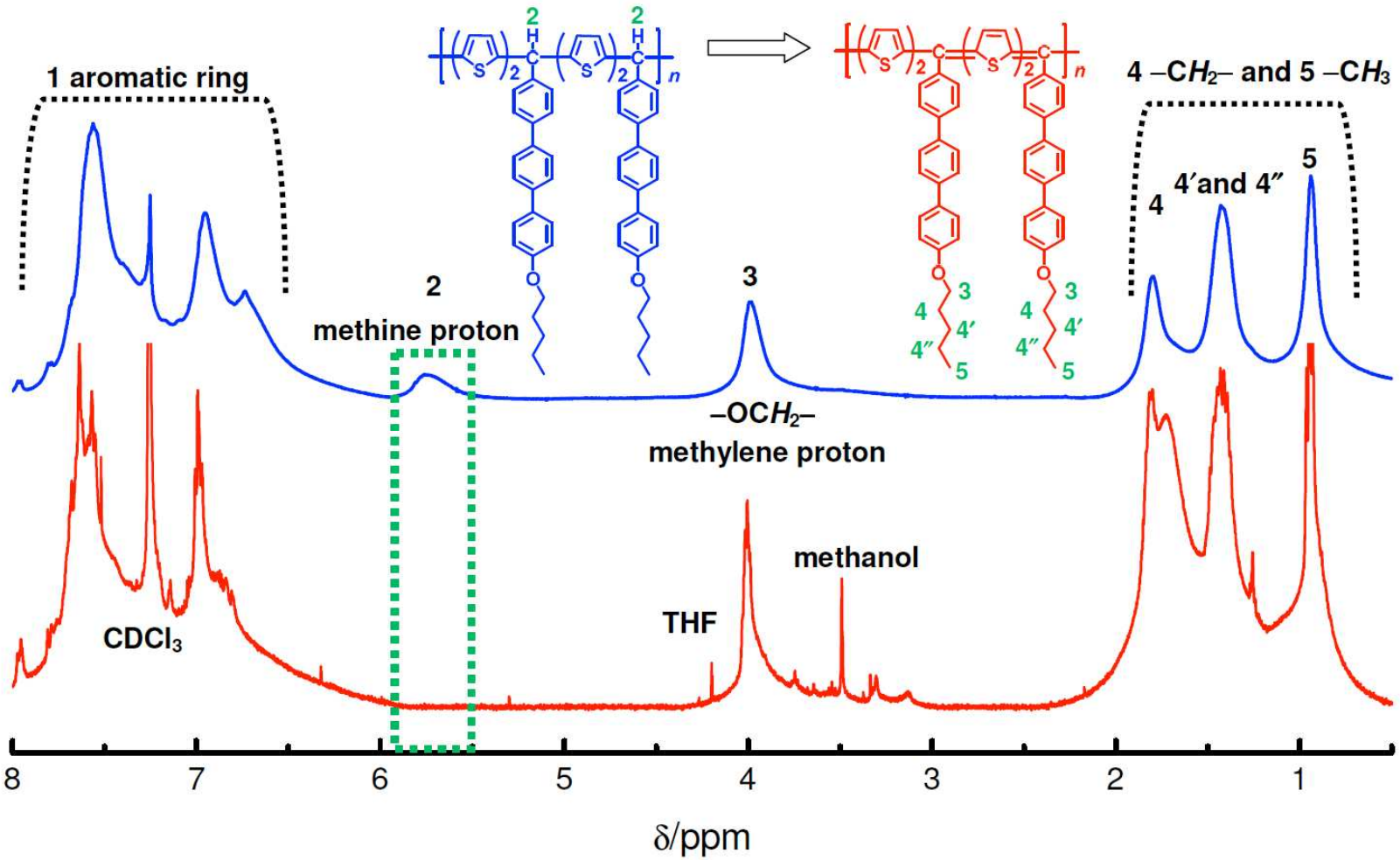

Figure 1. ^{1}H-NMR spectra of **Poly-2PB** (blue line) and **Poly-2PQ** (red line) in $CDCl_3$. The methine proton signal at ca. 5.8 ppm is indicated with a green dotted line box.

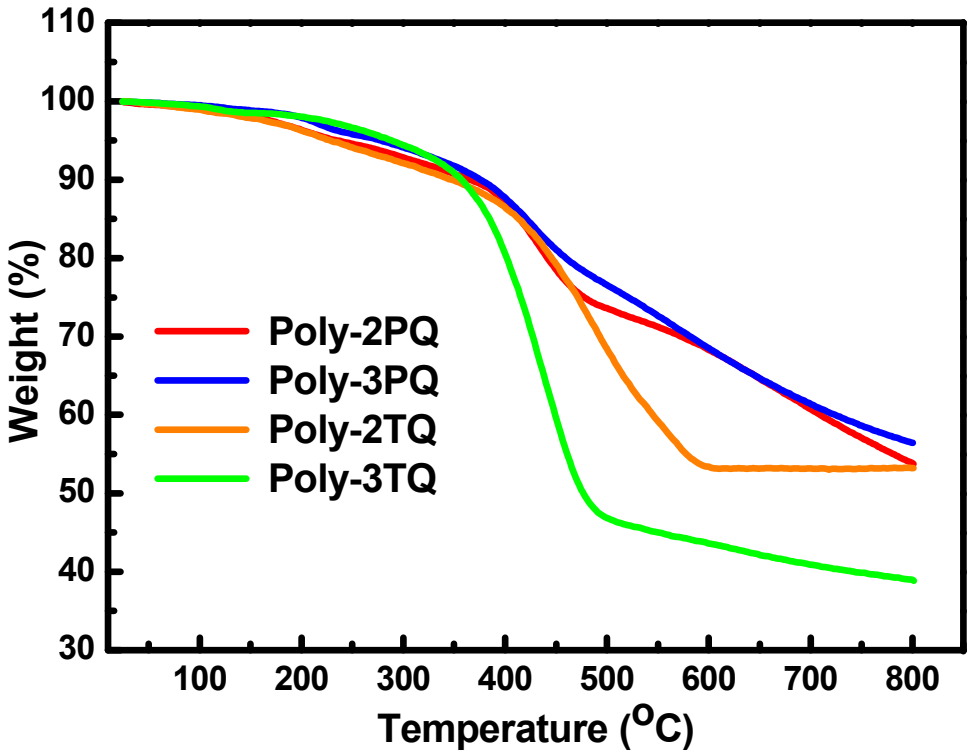

Figure 2. TG plots of quinoidal polymers (**Poly-2PQ**, **Poly-3PQ**, **Poly-2TQ**, and **Poly-3TQ**) with heating rate of 10 °C/min in N_2.

Table 1. Polymerisation results of **Poly-2PB**, **Poly-3PB**, **Poly-2TB** and **Poly-3TB**.

Polymer	M_n	M_w	M_w/M_n	D.P.[a] (T.U.)[b]
Poly-2PB	5,100	7,400	1.45	10 (20)
Poly-3PB	5,000	8,000	1.60	9 (27)
Poly-2TB	2,400	2,700	1.17	3 (6)
Poly-3TB	2,600	2,800	1.08	3 (9)

a) D.P.: Degree of polymerisation

b) T.U.: Number of thienylene unit

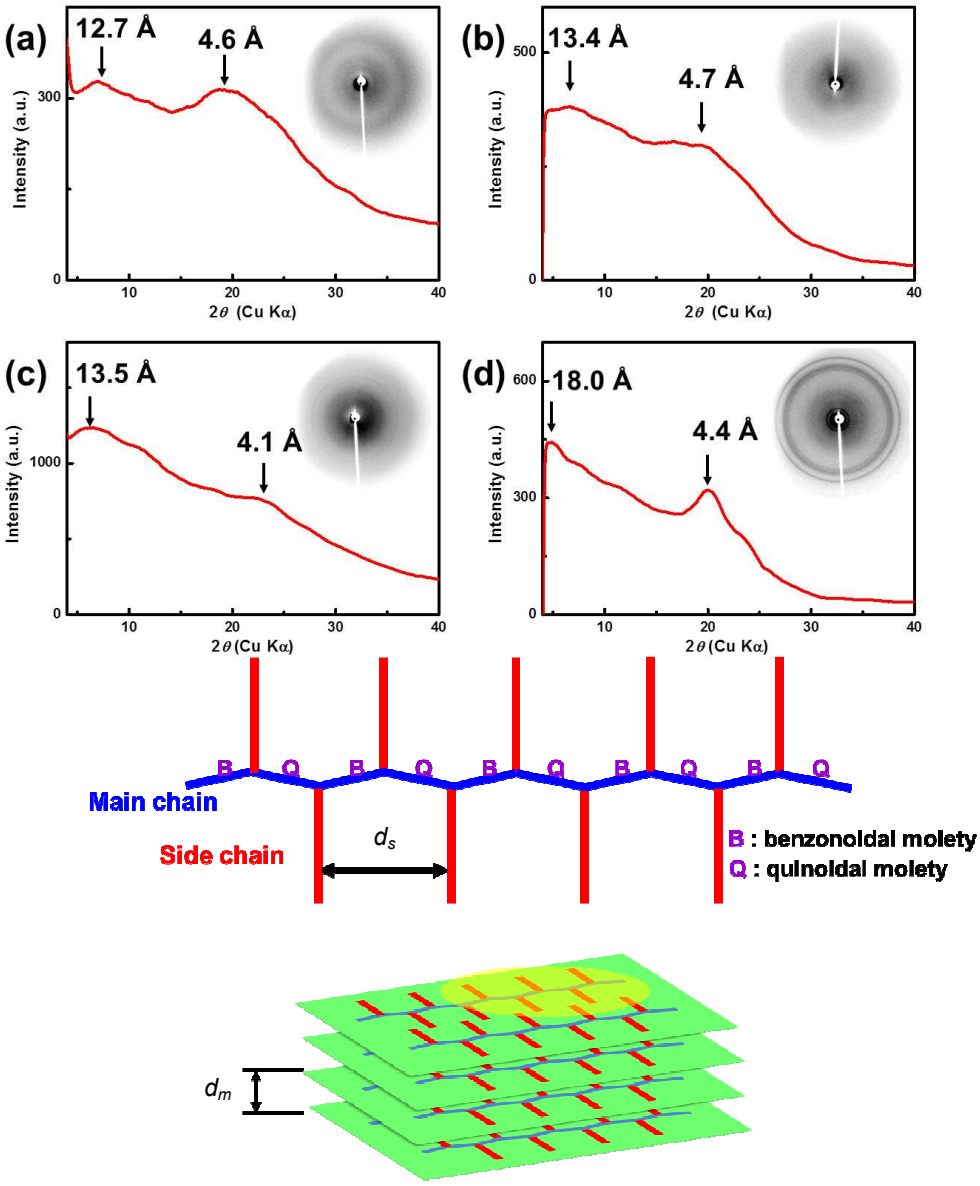

Distance (d_s) between next-neighbouring side chains

	Poly-2PQ	Poly-3PQ	Poly-2TQ	Poly-3TQ
calculated value:	11.3~14.6 Å	15.7~21.2 Å	14.5~18.2	18.2~24.1 Å
experimental value:	12.7 Å	13.4 Å	13.5 Å	18.0 Å

Distance (d_m) between π stacking polymer chains

experimental value:	4.6 Å	4.7 Å	4.1 Å	4.4 Å

Figure 3. (upper) X-ray diffraction patterns of (a) **Poly-2PQ**, (b) **Poly-3PQ**, (c) **Poly-2TQ**, and (d) **Poly-3TQ**. (lower) Schematic representation of quinoidal polymer. The distances between the next-neigbouring site chains were evaluated by molecular mechanics calculations using MMFF94 force field program (Spartan 10), where the quinoidal polymers with 10 repeating units consisting of alternative benzonoidal and quinoidal moieties were employed as model systems.

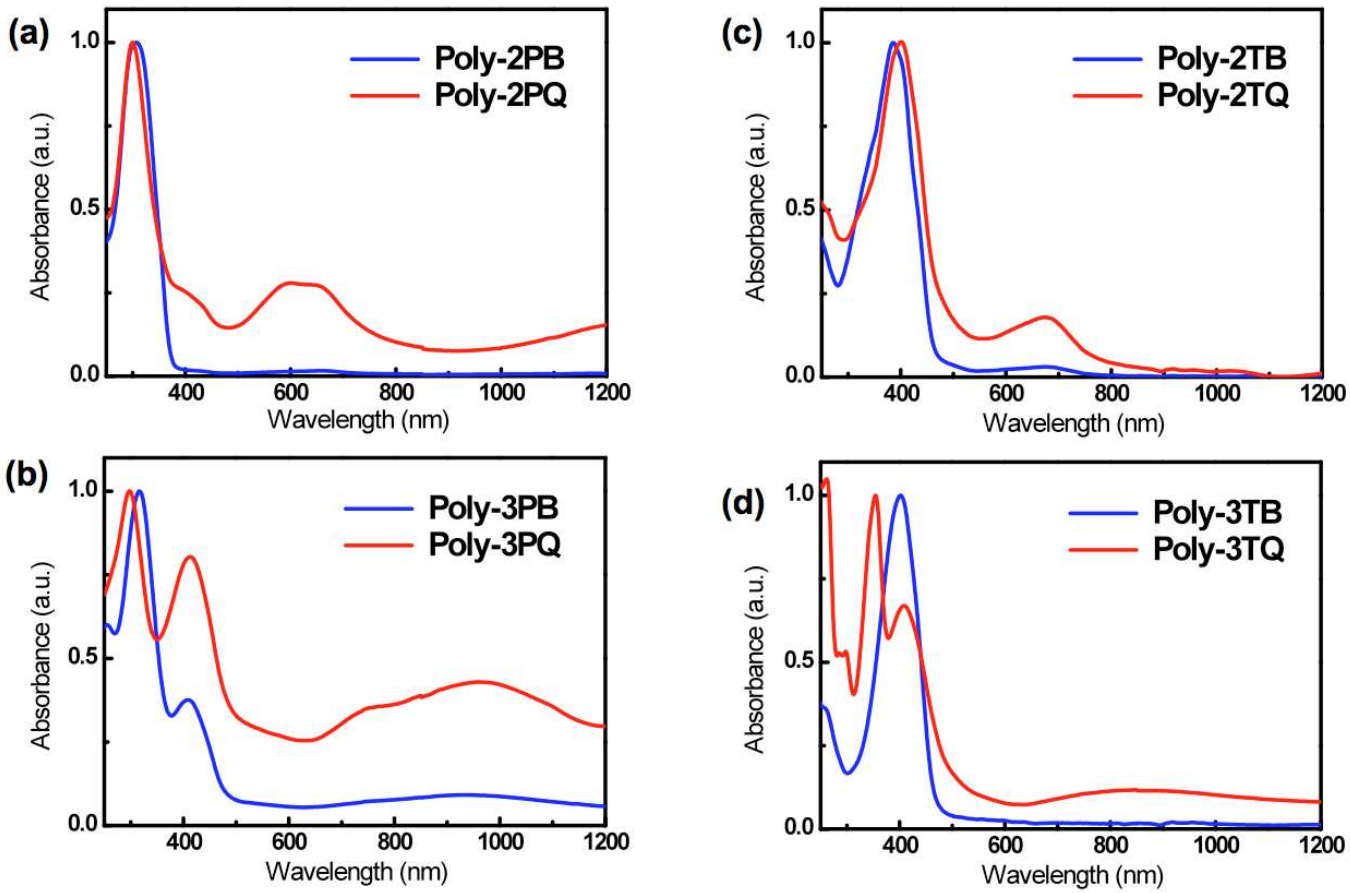

Figure 4. UV-Vis-NIR absorption spectra of (a) **Poly-2PB** and **Poly-2PQ**, (b) **Poly-3PB** and **Poly-3PQ**, (c) **Poly-2TB** and **Poly-2TQ** and (d) **Poly-3TB** and **Poly-3TQ** in $CHCl_3$. The blue and red lines in the spectra indicate the benzonoidal and quinoidal polymers, respectively.

Table 2. Optical and electrochemical bandgaps of **Poly-2PQ**, **Poly-3PQ**, **Poly-2TQ** and **Poly-3TQ**.

Polymer	UV-vis		Optical bandgap	Potential [a]		Energy level		Electrochemical bandgap
	λ_{max} (nm)	λ_{onset} (nm)	(eV)	$E_{potential}$ (V;vs Ag/Ag^+)	E_{onset} [b] (V;vs Ag/Ag^+)	HOMO (eV)	LUMO (eV)	(eV)
Poly-2PQ	600	750	1.7	+1.63, –1.23	+1.37, –0.80	–5.7	–3.5	2.2
Poly-3PQ	970	1560	0.8	+0.74, –1.67	+0.39, –1.22	–4.7	–3.1	1.6
Poly-2TQ	680	810	1.5	+1.03, –1.74	+0.38, –1.24	–4.7	–3.0	1.7
Poly-3TQ	890	1600	0.8	+0.85, –1.36	+0.23, –0.95	–4.5	–3.3	1.2

a) Reduction and oxidation potentials measured by cyclic voltammetry.

b) The reduction and oxidation potentials were evaluated assuming that the absolute energy level of ferrocene/ferrocenium is below 4.8 eV in a vacuum.

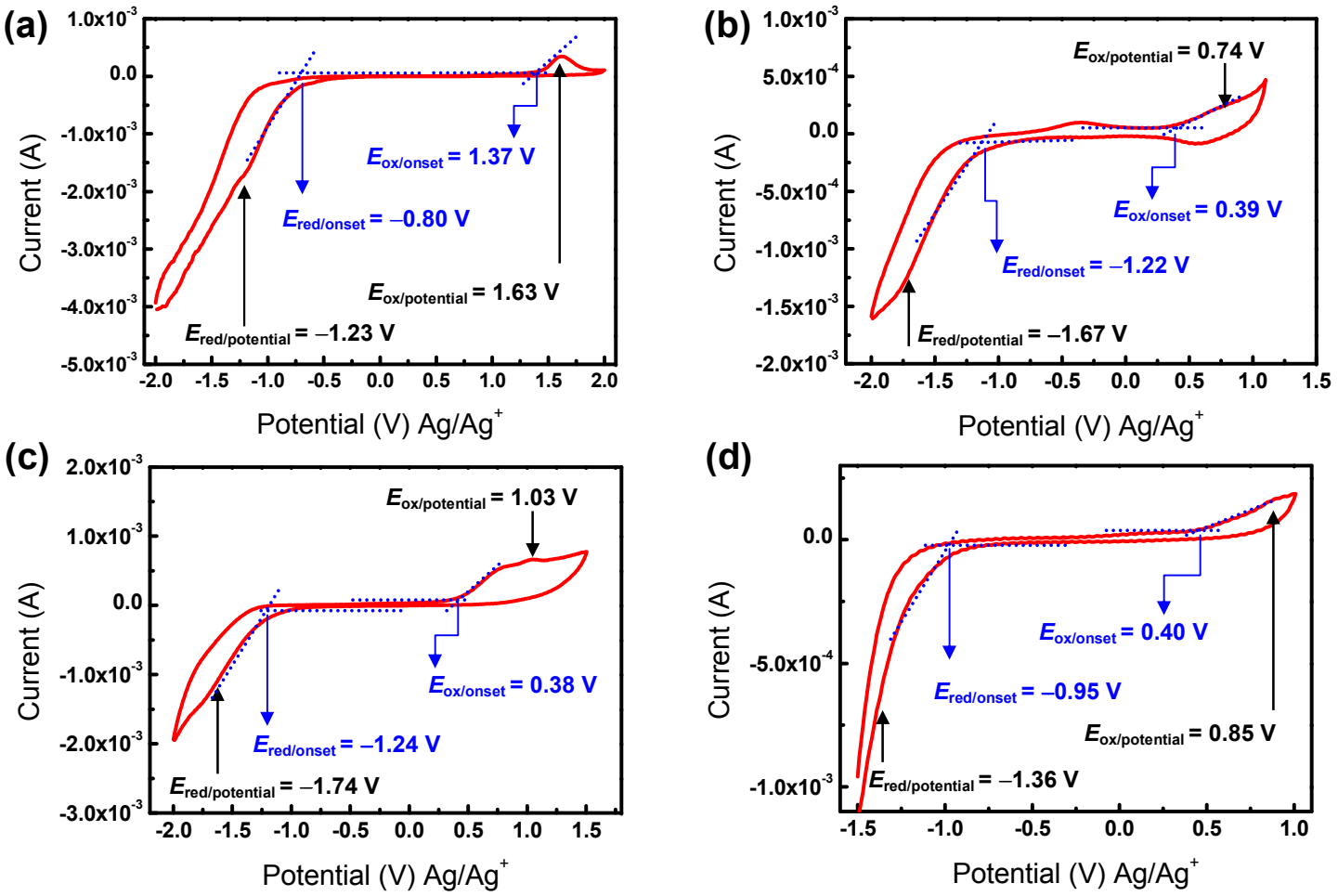

Figure 5. Cyclic voltammograms of (a) **Poly-2PQ,** (b) **Poly-3PQ**, (c) **Poly-2TQ**, and (d) **Poly-3TQ** films on a platinum electrode in acetonitrile containing 0.1 M tetrabutylammonium perchlorate (TBAP) measured with a scan rate of 10 mV/sec.

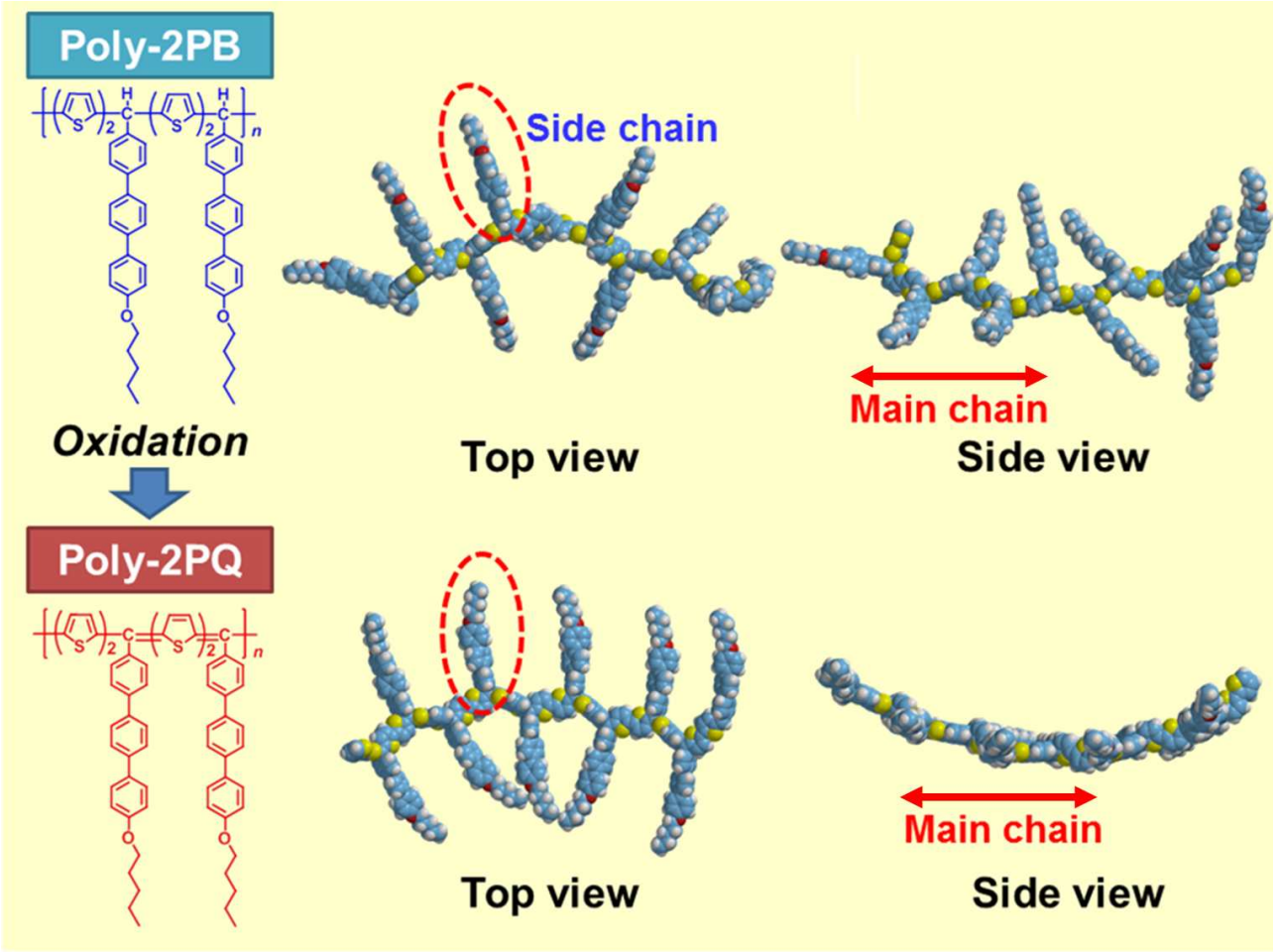

Figure 6. Three-dimensional models for the benzonoidal polymer, **Poly-2PB** (above) and the quinoidal polymer, **Poly-2PQ** (below).

Table 3. Surface resistance and electrical conductivity of quinoidal polymer films

Polymers	Thickness (nm)	Surface resistance (Ω/sq.)		Electrical conductivity (S/cm)	
		Intact	I_2 doped	Intact	I_2 doped
Poly-2PQ	167.0	6.3×10^{10}	3.0×10^{9}	9.5×10^{-7}	2.0×10^{-5}
Poly-3PQ	132.3	5.1×10^{11}	1.8×10^{10}	1.5×10^{-7}	4.1×10^{-6}
Poly-2TQ	–[a]	–	–	–	–
Poly-3TQ	205.8	3.5×10^{13}	2.1×10^{10}	1.4×10^{-9}	2.3×10^{-6}

a): No film of **Poly-2TQ** was obtained.

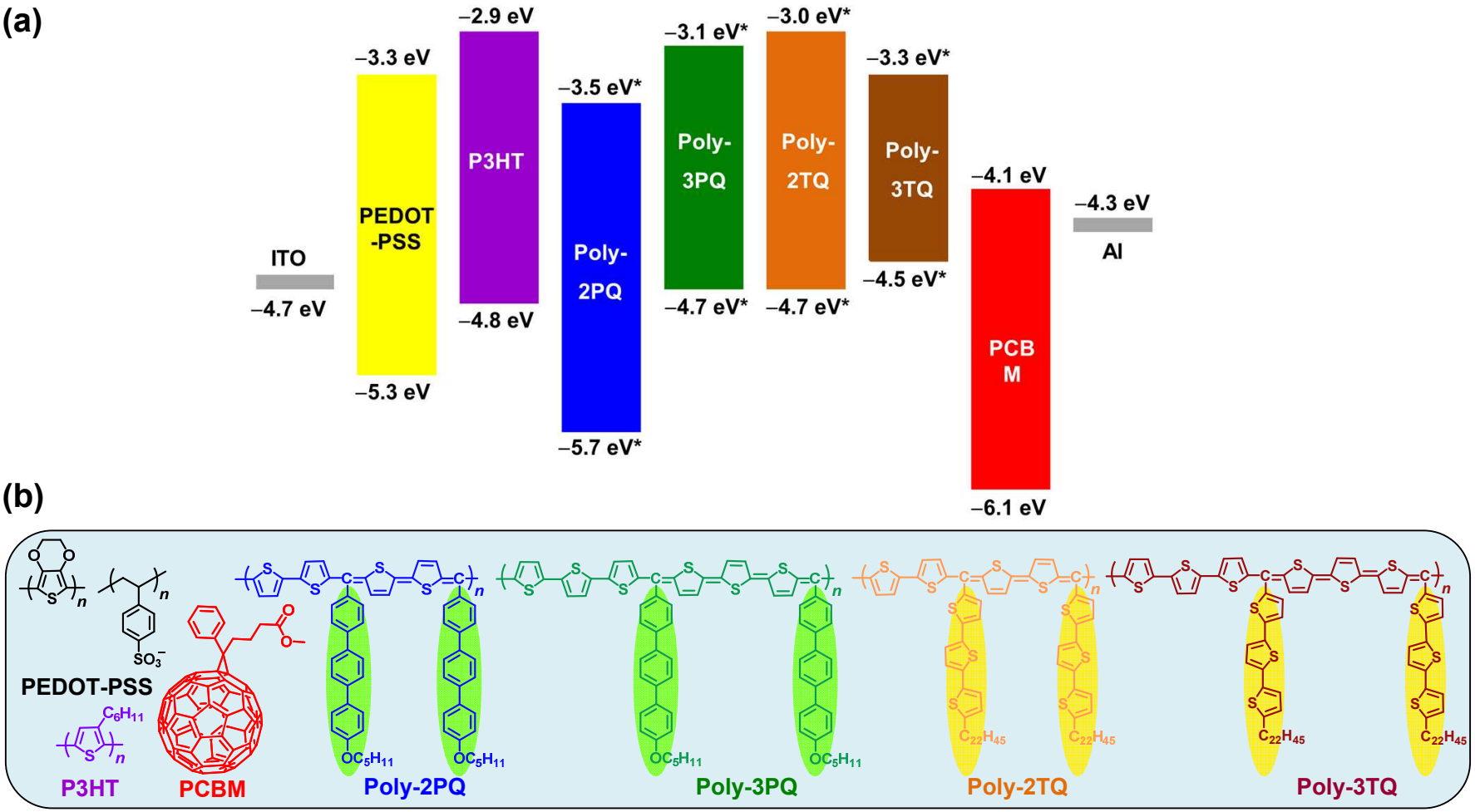

Figure 7. (a) Comparison of energy levels between **P3HT**, quinoidal polymers, and **PCBM**. (*): HOMO and LUMO levels of the quinoidal polymers were measured from cyclic voltammograms. (b) The molecular structure of **PEDOT-PSS** and **PCBM,** and polymer structures of **P3HT**, **Poly-2PQ**, **Poly-3PQ**, **Poly-2TQ**, and **Poly-3TQ**.

TOC (Table of Contents)

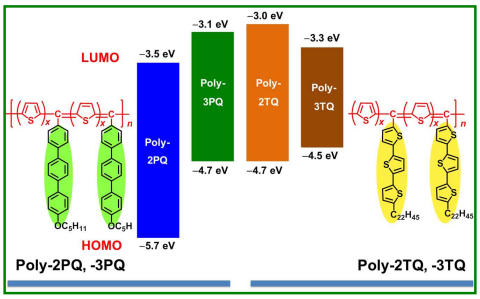

Novel low bandgap poly(thienylenemethine) derivatives bearing terphenylene moieties in the side chains were synthesised. The bandgaps were controlled by introducing quinoidal structures into the benzonoidal main chains.